Microstructure and Mechanical Characterization Study in the IN718/BNi-2/316L Joint by Transient Liquid Phase Bonding Process

M. Salmaliyan*, M. Shamanian

Department of Materials Engineering, Isfahan University of Technology, Isfahan, 84156-83111, Iran

*Corresponding author: E-mail: salmaliyan.mehran@gmail.com

Abstract

In this research, the relationship among TLP bonding microstructures, mechanical properties and fracture mechanism of IN 718 / BNi-2 /AISI 316L joint was studied. In the first step, by changing TLP variables e.g. time and bonding temperature in the range 30-60 min and 950-1050^{0}C respectively, characteristics of each type of microstructures including formation of destructive phases and homogeneity of microstructures were studied. In the second step, in order to investigate the mechanical properties and their fracture surface morphology, hardness and shear tests were accomplished. In the next stage, based on diffusion behavior of alloying elements, the relationship among microstructure, mechanical properties and fracture mechanism was studied. Results show that microstructures of bonding region were classified in three types. Type I: solid state bonding microstructure, Type II: Athermal – isothermal solidification microstructure, and Type III: isothermal solidification microstructure. It was observed that for each specific microstructure, there is one fracture mechanism or there are more that are dimples fracture resulting from precipitations within matrix, quasi-cleavage fracture resulting from dual microstructure of eutectic – isothermal solidification and dimple-tearing fracture resulting from tiny precipitations within bonding region. Copyright © VBRI Press.

Keywords: Diffusion bonding of IN 718, diffusion bonding of 316L, dissimilar welding, fracture mechanism, isothermal and Athermal solidification, transient liquid phase.

Introduction

Transient liquid phase (TLP) bonding is a combination of diffusion bonding and brazing that was introduced as an alternative method for joining super alloys [1]. On heating, the interlayer melts and the interlayer element (or a constituent of an alloy interlayer) diffuses into substrate materials, causing isothermal solidification. The result of this process is a bond that has a higher melting point than the bonding temperature [2-3]. One of the most important dissimilar joints is dissimilar joining of stainless steel to Ni-base super alloys. Bimetallic joints of stainless steel to Ni-based super-alloys are widely used in aerospace and power plant. Inconel 718 is a precipitation hardened Ni-based alloy widely employed in high temperature applications because of its excellent strength and corrosion resistance. In comparison to other Ni-based super-alloys, IN 718 is more resistant to age hardening due to the formation of coherent precipitation of Ni_3Nb. On the other hand, AISI 316L is an austenitic stainless steel widely used in intensive corrosion environments because of its excellent corrosion resistance. This alloy is one of the most usable materials of tubes in power plant industries [4-8]. Dissimilar weldments of SS-316L and IN718 alloy have been widely used in many engineering applications such as chemical processing equipment, aerospace engine components, power plants, and oil and gas industries. One of the most common applications of this dissimilar bonding is in stirling engine [3-4].

A lot of investigations have been carried out on dissimilar joining of Ni-base super-alloy/austenitic stainless steel by researches in recent years [6-11]. In these researches, microstructure of bonding region, diffusion-affected zone and some mechanical properties e.g. hardness and shear strength have been studied almost entirely. In TLP bonding of IN718, because of alloying elements diffusion, different intermetallic components form in the bonding region and DAZ region. These intermetallic components have different behaviors against shear loading that lead to different fracture modes and as a result, fracture mechanism varies. Todays, some new research for reducing of the intermetallic effects has been applied a new form of filler metal [6, 7]. However, a few studies in relation to relationship between bonding microstructure and fracture toughness have been conducted.

This research first aims to study the microstructure of IN 718 / BNi-2 / 316L, which is obtained by changing the process variables. This step consists of morphology and characterization studies in bonding region, too. In the second step, mechanical properties of

bonding region, fracture behavior and fracture morphology of bonding region will be studied, and in the final step, it aims to find a relationship between microstructure, mechanical properties and fracture behavior. The novelty of this research can be divided into several parts that include: a) study of weld ability of IN718 / BNi-2 / 316L joint by TLP process, and b) creation of a meaningful relationship between the microstructure of the IN718 / BNi-2 / 316L joints, the mechanical properties and the behavior of the fracture of the joints, which has not been investigated so far.

Material and method

Nickel-based super-alloy IN-718 and austenitic stainless steel AISI 316L are used as base metals and BNi-2 foil as intermediate bonding layer whose chemical compositions have been shown in **Table 1**. The base metal samples were prepared by wire cutting method in the form of rectangular cube bars with dimensions of 10×10×5 mm. Thickness of BNi-2 foil was 50μm. Samples before diffusion bonding were prepared by grinding on SiC grit papers up to 400, and then they were assembled by a fixture made by two pieces of plate with two bolts in such a way that clamping force in each bolt was applied about 1140 N. TLP diffusion bonding of IN 718 / BNi-2 / AISI 316L was carried out in a furnace with heating rate of $8.75 \frac{℃}{min}$ under a vacuum of approximately 10^{-5} torr. Bonding temperature and time have been selected from 950, 1000 and 1050 ℃ and 30, 45 and 60 min, respectively.

A simple carbon steel (St37) fixture was used to fix the coupons in order to hold this sandwich assembly and reduce metal flow during the TLP operation. **Fig. 1** shows TLP bonding fixture. After diffusion bonding, coupons of 10×10×5 mm were cut perpendicular to the bonding line, and then microstructural observation was made on the cross-sections of specimens using an optical microscope (OM) and scanning electron microscope (SEM). For this purpose, the samples were subjected to the standard metallographic preparation procedure starting by grinding on SiC grit papers up to 2400, followed by polishing in alumina particle suspension (0.05 and 0.01 μ m size), and then they were ultrasonically cleaned in distilled water bath. Finally, base metals were etched with different etchants. The side of IN 718 was etched by electro etch method with 5 mL H2PO4, 47 mL H2SO4, 41 mL HNO3 etchant and the side of AISI 316L was etched by chemical method with 33 mL HCl, 33 mL HNO₃, 33 mL H₂O etchant. In addition to using optical microscope for observation of bonding microstructure, scanning electron microscope (SEM) model XL 30

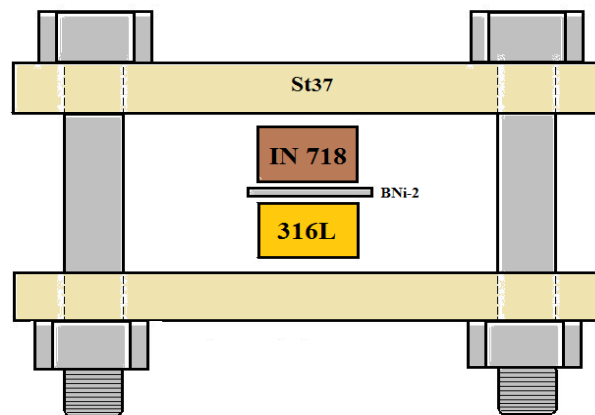from Philips Corporation was used too in order to observe the fracture surfaces.

Fig. 1. IN718/BNi-2/316L Sandwich assembly with a carbon steel fixture.

At room temperature, the shear strength of the bonds was evaluated using a shear test fixture with a crosshead speed of 1 mm/min. Shear test fixture has been shown in **Fig. 2**. As can be seen, the fixture has been designed in such a way that bonding region was placed in the center of fixture and as a result *pure shear* occurred during shear testing. Vickers micro hardness measurement was carried out using a Bohler micro-hardness machine. The load was set at 200 gr for 25 s dwell time. The hardness test was done in three different bonding regions including: base metals, diffusion affected zone and bonding regions.

Characterization of formed phases in the centerline of the bonding region and base metals was analyzed using EDS with model EDAX silicon drifted. Finally, grain size number was measured by Imagej software.
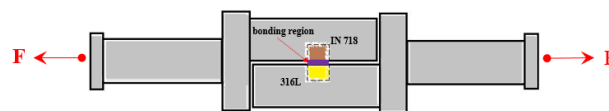

Fig. 2. Shear test fixture.

Results and discussion

Microstructure IN718 / BNi-2 /316L joints

Fig. 3 to **Fig. 5** show microstructures of IN 718 / BNi-2 / AISI 316L joints at bonding time and temperature of 30, 45 and 60 min and 950, 1000 and 1050 ℃, respectively. Before studying the bonding microstructure, some distinct microstructures were described in the following sections:

– *Isothermal Solidification Zone (ISZ):* ISZ which usually consists of a solid solution phase. Compositional change induced by inter diffusion

Table 1. Chemical composition of base metals (IN718 & 316L) and BNi-2 interlayer.

Material	Ni	Cr	Mo	Si	B	Mn	C	Nb	Ti	P&S	Al	Fe
IN 718	50	18	3	0.35	-	0.35	0.08	5	1	<0.03	0.5	-
316L	12	16	2.5	1	-	2	0.03	-	-	<0.07	-	Bal.
BNi-2	82.4	7	-	4.5	3.1	-	-	-	-	-	-	3

between substrate and interlayer during holding at a constant bonding temperature is the driving force for isothermal solidification. As a result of the absence of solute rejection at the solid/liquid interface during isothermal solidification under equilibrium, formation of the second phase is basically prevented [**8**].

– *Athermal Solidification Zone (AFZ):* Athermal solidified zone (ASZ), which usually consists of eutectic micro constituents. This zone is formed due to insufficient time for isothermal solidification completion. Cooling is the main driving force for Athermal solidification (i.e. non-isothermal solidification) [**8**].

– *Diffusion Affected Zone (DAZ):* In this region, the microstructure is influenced by the diffusion of MPD elements into the BM. Therefore, the microstructure of this region consists of secondary phase precipitates (mainly boride in the case of B-containing filler alloys) [**9**].

First of all, **Fig. 3 a), b), c)** shows the microstructure of IN 718 /BNi-2/316L joint at bonding temperature 950 ℃ for 30, 45 and 60 min. As can be seen, by increasing the bonding time at constant temperature, bonding region width is nearly constant, but diffusion affected zone (DAZ) increases. It is necessary to mention that because bonding temperature is lower than melting point of interlayer (melting point of interlayer is around 977 ℃), diffusion bonding is accomplished at solid state. In this situation, by increasing the bonding time just inter diffusion between components increases.
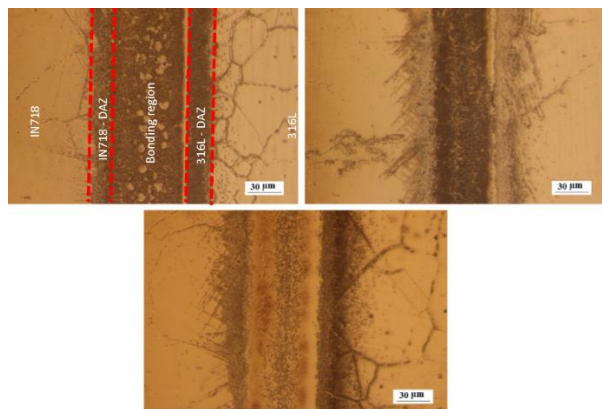

Fig. 3. Optical microscopic image of IN 718/ BNi-2 /AISI 316L joint that have been done at –a) bonding temperature 950 ℃ for 30 min, b) bonding temperature 950 ℃ for 45 min, c) bonding temperature 950 ℃ for 60 min.

Among the characteristics of these types of microstructures are the following: Bonding has been made in the form of solid state and not in the form of TLP, the width of bonding region is the same as that of the interlayer filler metal, bonding region morphology of this microstructure at low bonding time is heterogonous, and in the center of bonding, there are island regions with different chemical compositions.

Finally, intermetallic components in the DAZ region on IN718 side have acicular shapes but the DAZ region on 316L side has spherical shapes.

Fig. 4 a, b, c shows the microstructure of IN 718 /BNi-2/316L joint at bonding temperature 1000℃ for 30, 45 and 60 min. In this temperature, interlayer melts and leads to an increase in the diffusion rate. As can be seen, at short bonding time, interlayer alloying elements did not have enough time for diffusion into base metal. In addition, because of very low solubility of boron in Ni and low partition coefficient of boron in Ni [**8**], boron is rejected to adjacent liquid causing the chemical composition of this region to go to the eutectic composition. With progressing of solidification, binary/ ternary eutectic is formed between γ phase (Ni-rich solid solution) and nickel boride/silicide. This form of solidification is characteristic of Athermal Solidification (AS). On the other hand, by increasing the bonding time, thickness and continuity of AS at bonding region reduce and isothermal solidification (IS) increases.
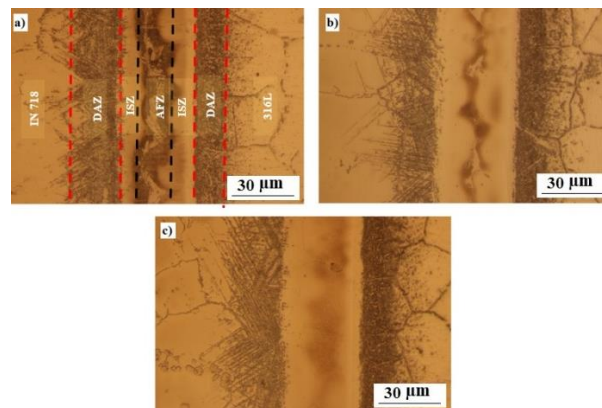

Fig. 4. Optical microscopic image of IN 718 / BNi-2 / AISI 316L joint that have been done at –a) bonding temperature of 1000 ℃ for 30 min b) bonding temperature of 1000 ℃ for 45 min c) bonding temperature of 1000 ℃ for 60 min.

Among the characteristics of these types of microstructures are the following: both Athermal and isothermal solidifications have been observed, by increasing the bonding time, eutectic and dendritic regions volume reduce, the width of bonding and DAZ regions have also increased compared to the previous microstructures. Finally, acicular and spherical intermetallic components formed on DAZ regions are similar to previous microstructures with the difference that length and width are more than those in the previous microstructures.

Fig. 5a, 5b shows microstructure of IN 718 /BNi-2/316L joint at bonding temperature 1050 ℃ for 30 and 45 min. Similar to joining condition at bonding temperature 1000℃ and 30 min, solidification mode at bonding temperature 1050℃ and 30 min is the combination of AS and IS. In this bonding temperature, isothermal solidification was completed at bonding time 45 min. In other words, not only was the bonding time enough, but also diffusion affected zone was wider than

other samples. In fact, after completing IS, alloying elements e.g. melting point depressants (MPD) diffused into base metals and intermetallic compounds were formed lead to an increase in the DAZ region.
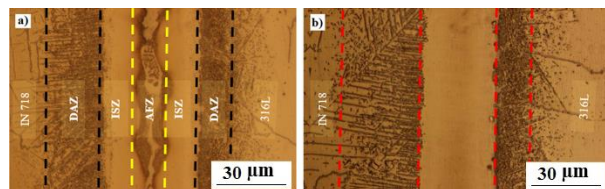

Fig. 5. Optical microscopic image of IN 718 / BNi-2 / AISI 316L joint that have been done at–a) bonding temperature of 1050 ℃ for 30 min and b) bonding temperature 1050 ℃ for 45 min.

Among the characteristics of these types of microstructures are the following: full isothermal solidification was obtained in this microstructure, the width of bonding and DAZ regions have increased compared to both types of previous microstructures. Finally, acicular and spherical intermetallic components formed on DAZ regions are similar to previous microstructure, but their length and width are more than those in both types of previous microstructures.

All of bonding microstructures that were shown in **Fig. 3** to **Fig. 5** can be categorized in three distinct microstructures consisting of: *Type I-* solid state diffusion bonding microstructure, *Type II-* Athermal & isothermal solidification bonding microstructure and *Type III-*isothermal solidification bonding micro-structure. These three distinct microstructures were shown in **Fig. 6**. Classification of these microstructures is based on time & bonding temperature. If temperature be insufficient, diffusion bonding occurs at solid state; on the other hand, if bonding time at right temperature be insufficient, Athermal & isothermal solidification bonding microstructure can be seen. Finally, if time and bonding temperature were selected in order to achieve optimal microstructure and mechanical properties, isothermal solidification bonding microstructure could be achieved. This categorization can be useful to better identify the fracture mechanism.
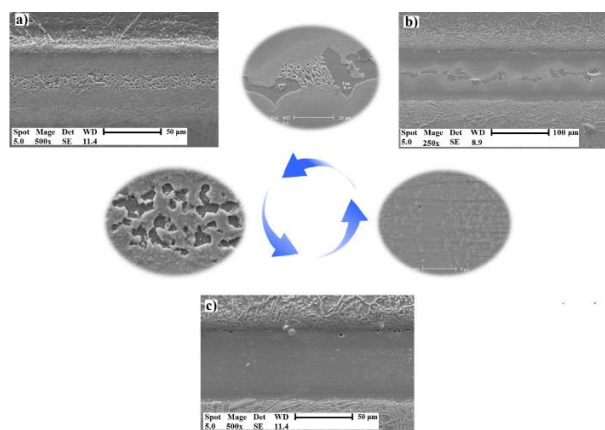

Fig. 6. Three distinct microstructures of IN 718/ BNi-2/ AISI 316L joint – a) Type I: solid state diffusion bonding microstructure b) Type II: Athermal & isothermal solidification bonding microstructure c) Type III: isothermal solidification bonding microstructure.
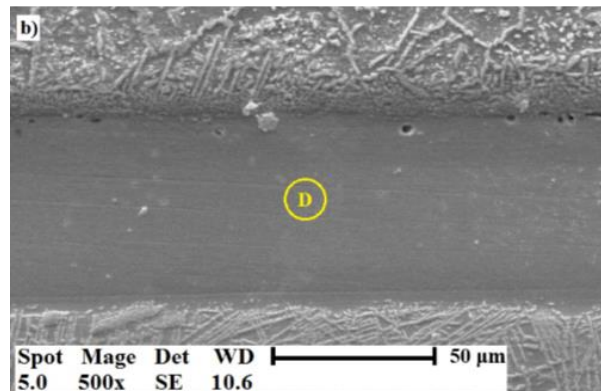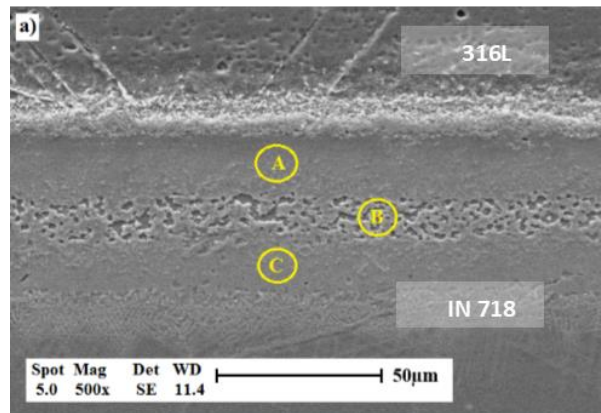

Fig. 7. Characterization of TLP diffusion bonding of IN 718 / BNi-2 / 316L – a) solid state diffusion bonding microstructure b) isothermal solidification bonding microstructure.

Table 2. Result of EDX elemental analysis of type I and type II microstructure.

Element (%wt.)	A	B	C	D
B	5.40	3.6	5.34	3.57
Si	2.81	2.88	2.93	2.67
Nb	2.31	2.27	2.49	2.18
Ti	0.58	0.49	0.71	-
Cr	9.15	8.64	7.93	9.10
Fe	6.99	7.17	7.41	8.12
Ni	72.76	74.12	73.17	74.36

Bonding region characterization

Fig. 7 to **Fig. 11** show chemical compositions of IN 718 / BNi-2 / AISI 316L joints at different bonding conditions. Points A, B and C in **Figs. 7a, b** and **c** show places of EDX elemental analysis of Type-I microstructure. **Fig. 7d** shows place of EDS elemental analysis of bonding region in Type III microstructure. **Table 2** shows chemical composition of Type I & Type III microstructures. It is observed that Ni and boron (B) diffuse to base metal from interlayer and Fe, Cr, Ti, Si and Nb diffuse to bonding region from base metals. In spite of being semi-quantities of EDS analysis, valuable data were achieved on diffusion behavior of elements. Based on basic laws around diffusion in metals, it is clear that diffusion driving force is chemical potential and not concentration gradient [**10**]. By comparing the chemical composition of bonding region, BNi-2 interlayer and base metals, it was observed that the amount of Si in bonding region increases. This

paradoxical behavior is reputed to uphill diffusion. This observation shows chemical potential and concentration gradient are not aligned for Si component. This observation is a little different for Cr, Ni and Fe. For example, the amount of Fe in BNi-2 interlayer before joining was 3 %wt. but after diffusion bonding, it was increased up to 7 %wt. On the other hand, the amount of Cr in BNi-2 interlayer was lower than both base metals; and after bonding, its amount increased. In other words, chemical potential and concentration gradient are aligned for Cr, Fe, Nb, Ti, B and Ni components. Another point to be said is about the central bonding region in Type-I microstructure. As can be seen by comparing the EDX chemical analysis of points A, B and C, concentration of components B, Si, Ni and Cr is different in these regions. The difference in the concentration of these regions will have a huge effect on the mechanical behavior and fracture of this type of microstructure.

Fig. 8 shows type II microstructure or Athermal & isothermal solidification bonding microstructure. There are two specific microstructures in this region consisting of: eutectic and single γ-phase microstructure. Single γ-phase microstructure consists of two regions: single γ-phase and Si-rich dendritic shape islands. The size of dendritic shape islands is variable from center of bonding region to bonding / base metal interface. In addition to this, the size of dendritic shape islands decreases by being away from the center of bonding region. In **Fig. 8**, these dendritic shape islands are specified by <u>**A**</u> Capital letter. In addition to this, **Table 3** shows chemical composition of Type II Athermal & isothermal solidification bonding microstructure. As it can be seen from **Table 3**, point of <u>**A**</u> shows that these islands are Si-rich components. These dendritic islands have been noticed in other investigations, too [2-6-9].
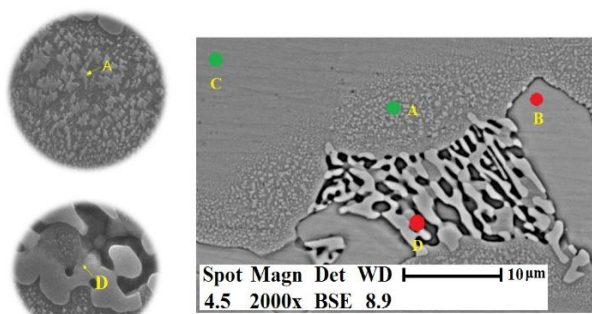

Fig. 8. Characterization of TLP diffusion bonding of IN 718 / BNi-2 / 316L - Athermal & isothermal solidification bonding microstructure.

Table 3. Result of EDX elemental analysis of type III microstructure.

Element (%wt.)	A	B	C	D
B	3.62	3.62	3.02	7.28
Si	9.4	2.25	2.06	9.45
Nb	3.23	3.23	2.80	23.60
Ti	0.76	0.76	0.74	1.05
Cr	10.80	11.03	12.12	1.79
Fe	10.2	10.98	11.03	1.87
Ni	62.25	68.13	68.24	54.96

Eutectic microstructure consists of two specific regions that include: boride/silicide compounds and single γ-phase. Points D and B in **Fig. 8** show chemical composition of binary/ternary eutectic microstructure. As can be seen, point B is an Ni-rich region. At higher magnification of point D, this point consists of γ-single phase, Si-rich and B-rich compounds. Because of high volume fraction of Si and B-rich compounds in this region, hardness of this region is more than other regions. Finally, chemical composition of point C shows an Ni-rich region with small amounts of Cr, Si and Fe.

Hardness characteristics of the TLP bonds

Fig. 9 shows the hardness profile of bonding regions that consist of: base metals, diffusion affected zone (DAZ) close to base metal, DAZ close to bonding region and bonding region. It should to say that hardness test for each region was carried out three time. As can be seen in **Fig. 9**, the hardness of base metals does not have a significant difference, however, it was observed that with an increase in time and temperature from 950 to 1050ºC and 30 to 60 min, respectively, the hardness of base metals slightly decreases. The reason for this latter result can be related to grains growth or precipitations growth in IN718 super-alloy. **Fig. 10** shows grain size of IN718 alloy for two different bonding conditions of 950ºC for 30 min (a) and 1050ºC for 45 min (b). By using image j software, grain size measurement has been done. After measurement, average grain sizes of samples a) and b) were nearly 60 and 160 µm, respectively.
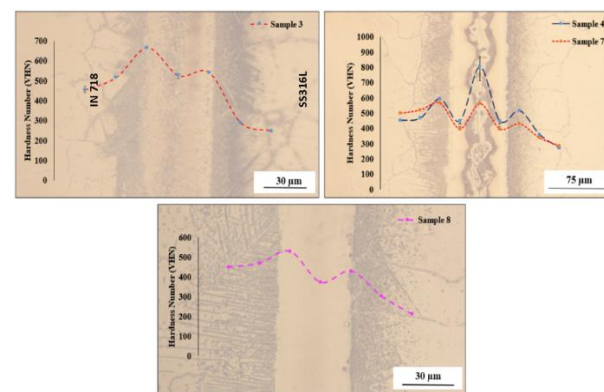

Fig. 9. Hardness profile of IN 718 / BNi-2 / 316L joint at - a) solid state diffusion bonding microstructure b) athermal & isothermal solidification bonding microstructure for two sapmle with different bonding variables (bonding condition for sample 4 and 7, respectively: 30 min at 1000ºC, 30 min at 1050ºC) c) isothermal solidification bonding microstructure.

As can be seen in **Fig. 9**, a) hardness number in DAZ region is more than that of base metals. This result is because of formation of Boride precipitations in this region. In addition, hardness of DAZ at 316L side is lower than DAZ at IN718 side. This observation can be studied from two aspects: first, primary hardness of IN718 super-alloys is more than that of 316L alloy; therefore, after formation of Boride precipitation, the

hardness increases more than before TLP bonding. Secondly, Boride precipitations at IN718 side are Nb, Ti and Ni base, but at 316L side are Cr, Fe and Ni base. Whereas characteristic of precipitations in either of both DAZ regions are slightly different; therefore, it causes hardness to vary [**12, 13**].

Fig. 9b shows hardness profile Type II microstructure with two samples at the same time, but different bonding temperatures. TLP bonding of Sample 4 was carried out at 1000 ℃ and 30 min, on the other hand, sample 7 was bonded at 1050 ℃ and 30 min. It can be seen that DAZ regions hardness on both samples is similar to **Fig. 9a**, but in eutectic region, there are many difference. As can be seen, eutectic region hardness of sample 4 is much more than that in sample 7. The reason for this observation can be related to diffusion behavior. As regards, samples 4 and 7 are different on bonding temperature, and it is clear that with an increase in temperature, diffusion increases. Due to increase in diffusion, more MPD elements diffuse towards base metals. Therefore, during Athermal solidification, boron and Si did not have sufficient time to diffuse in liquid state leading to form less hard eutectic products (borides and silicide).

Fig. 9c shows hardness profile type III or isothermal microstructure. Hardness number on base metals and DAZ region is nearly similar to type I and II microstructures, but it needs to be seen a little deep on ISZ hardness. As can be seen, bonding region hardness in ISZ is less than bonding region of Type I microstructure. This observation can be related to diffusion of MPD elements, too, since diffusion at melting state is more than solid state. Due to diffusion of MPD towards base metals, formation of hard and destructive phases at melting state occurred less than solid state. In this reason, type I microstructure hardness is more than type III microstructure hardness.
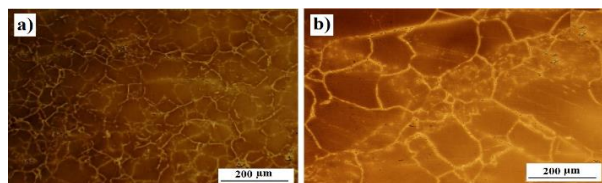

Fig. 10. Microstructure of IN718 at two different bonding conditions - a) 950℃ for 30 min, b) 1050 ℃ for 45 min.

Shear strength characteristics of the TLP bonding

Shear strength of three types of microstructures has been shown in **Fig. 11**. As can be seen, Type III microstructure has the most shear strength. The maximum shear strength that was measured was 480 Mpa. On the other hand, Type I & II microstructures nearly show the same shear strength 300 and 280 Mpa, respectively.

As regards, shear parameter of base metals are defined just in the form of shear module. For this reason, shear strength of bonding region could not be compared with strength of base metals. However, there is a general relationship between Young's modulus and

shear modulus based on non-compressible principle of a solid. Equations 1 and 2 show relationship of Young's modulus – shear strength and Young's modulus – shear modulus, respectively. By extracting shear strength and shear strain from **Fig. 11** and then putting them in equation 1, shear module can be calculated. As regards, shear strength and strain of bonding region are 475 Mpa and 2.3%, respectively, therefore, shear module is equal to 21 GPa.

$$G = \frac{Shear\ Strenght}{Shear\ Strain} = \frac{\sigma_s}{\varepsilon_s} \qquad (1)$$

$$E = 2 * G\ (1 + \nu) \qquad (2)$$

In the second step, by putting shear module in equation 2, bonding region of Young's modulus was calculated, too, that is equal to 55 Mpa. Because of complex composition in the bonding region, passion ratio of this region is not available in references. As regards, on the one hand, bonding region composition is Ni – rich, and on the other hand, passion ratio of most Ni alloys is nearly 0.29. In this study, bonding region Poisson's ratio was selected similar to Ni- base alloy.
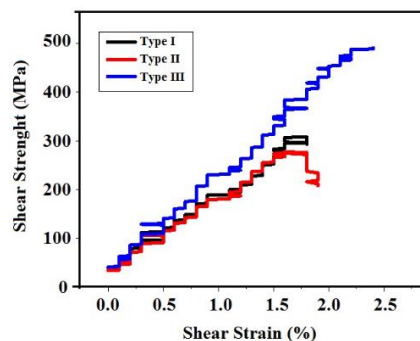

Fig. 11. Shear strenght of IN 718 / BNi-2 / 316L joint for three type microstructure-of solid state diffusion bonding microstructure (Type I), Athermal & isothermal solidification bonding microstructure (Type II), isothermal solidification bonding microstructure (Type III).

Table 4 shows the results of mechanical properties of base metals and bonding region in brief. *Exp.* and *Cal.* words in **Table 4** mean *experimental* and *calculated,* respectively. It is observed that both Young's modulus and shear modulus of bonding region are less than base metals. On the other hand, it is seen that shear strength of bonding region is more than AISI 316L, but less than IN718. Therefore, results show that strength of Type III is in the acceptable range and the reason for being low shear & Young's modulus is high shear strain and not being low shear strength.

Table 4. Mechanical properties base metals (IN 718 & AISI 316L) and bonding region.

Material	Yield strength (0.2 % offset) MPa	Tensile strength MPa	Shear strength MPa	Elastic modulus (GPa)	Shear modulus (GPa)	Poisson's Ratio
IN 718	1036 [14]	1240 [14]	720	211 [14]	81.4 [*Cal·*]	0.29
316L	190	540	370	200	78	0.28 [15]
Bonding region	-	-	480 [*Exp·*]	55 [*Cal·*]	21 [*Cal·*]	~ 0.29

Fracture characteristics of the TLP bonding

As can be seen in **Fig. 12**, fracture surface consists of deep dimples. Presence of these dimples on fracture surface shows one of the dominant fracture mechanisms, meaning *Dimple Fracture*. The red dashed circle in **Fig. 12c** shows deep dimples very well. In addition to the mentioned mechanism, in some regions, *flutes* and *TTS[1] mechanism* can be seen, too. Signs of flutes mechanism by red dashed line can be seen in **Fig. 12d**. Although Flutes was defined elongated grooves or voids that widely connect spaced cleavage, as seen in **Fig. 12d**, elongated voids connect tearing planes. These observations and fracture mechanisms can be analyzed in some respects:

− First, dimple fracture occurs when inclusion or precipitation has been in microstructure, since for nucleation of dimples, microstructures need to be heterogeneous to voids nucleated and growth from precipitation / matrix interface. Although diffusion bonding was carried out in solid state, it seems that there are some precipitations in bonding region.

− Second, hard precipitations should be formed in soft matrix.

In addition to the above observation, some shallow voids can be seen in **Fig. 12c**. The yellow dashed circle shows signs of TTS fracture mechanism. It seems that because of growth of dimples, material resistance decreases, and as a result, tearing becomes a dominant fracture mechanism.
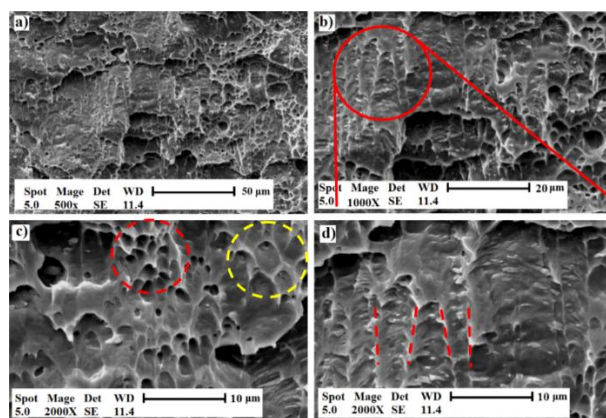

Fig. 12. Fracture surface of Type I microstructure a) overall image of fracture surface b) Flute fracture mechanism c) Dimple and TTS fracture mechanism, d) Flute mechanism.

Fig. 13 shows fracture surface of Type II microstructure at difference magnifications. As can be observed, fracture surface does not show plastic deformation and has stair shapes that have brittle fracture characteristics. Stair shape and planar fracture is one of the *cleavage fracture* mechanism signs that have been shown with red dashed elliptical in **Fig. 13c**. With a little carefulness, signs of *quasi cleavage* can be seen in **Fig. 13c** and **Fig. 13d**, since not only can planar fracture (**Fig. 13c**) be observed, but also the sign of

dimple fracture (**Fig. 13d**). Therefore, unlike Type I microstructure, fracture mechanism of Type II microstructure is *qusi cleavage*. The reason for these observations can be attributed to dual microstructure of Type II. In other words, Athermal solidification microstructure, because of containing brittle components, has planar fracture characteristics. On the other hand, isothermal solidification microstructure, because of containing γ phase, has soft characteristics that lead to dimple fracture.
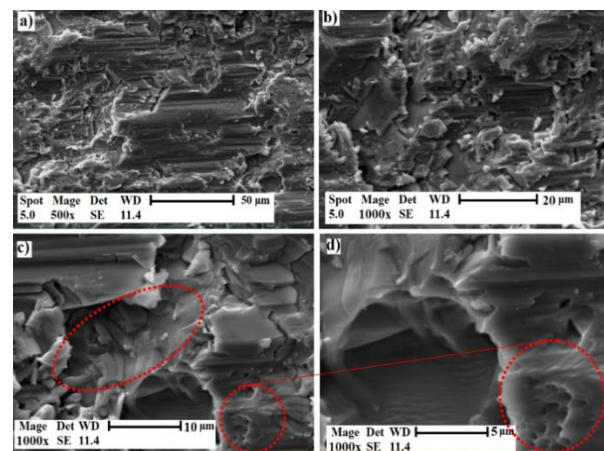

Fig. 13. Fracture surface of Type II microstructure a) & b) Overall image of fracture surface c) Cleavage fracture mechanism and d) Dimple fracture mechanism.

Fig. 14 shows fracture surface of Type III microstructure at difference magnifications. As seen, there are two difference fracture morphologies. Micron size voids in **Fig. 14b** and at higher magnifications. **Fig. 14d** shows dimples fracture mechanism. This fracture mechanism was reported by other researchers [**2**]. With a little carefulness on **Fig. 14c**, two separate regions can be seen. The right side of the red dashed line shows deep voids that are signs of dimple fracture, and the left side of red dashed line shows scattered shallow voids that are signs of TTS fracture mechanism. As mentioned in the previous section, TTS fracture mechanism, unlike dimple fracture mechanism, does not show much plastic deformation. This dual behavior of fracture mechanism can be explained in some ways.
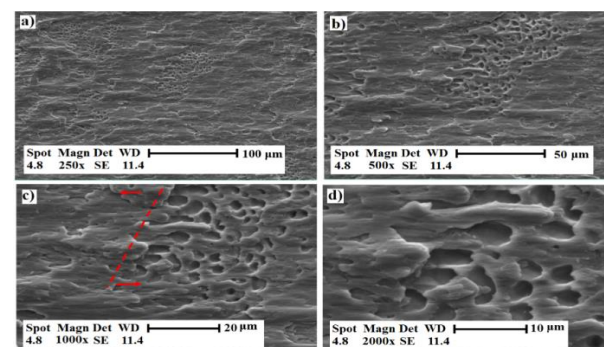

Fig. 14. Fracture surface of Type III microstructure a) & b) Overall image of fracture surface c) Dimple - Tearing fracture mechanism and d) Dimple fracture mechanism.
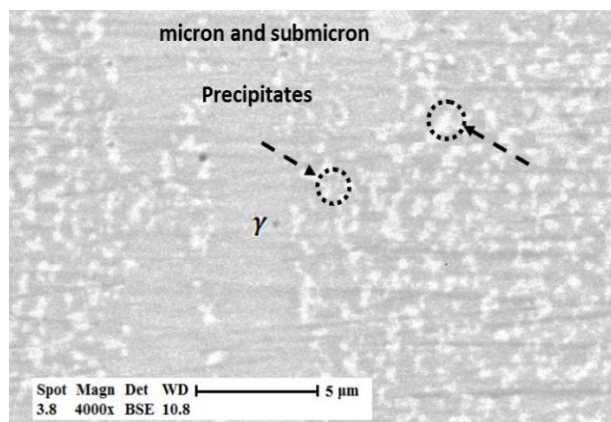
---

[1]tearing topography surface

Fig. 15. ISZ microstructure of TLP bonding of IN 718 / BNi-2 / 316L.

Although type III microstructure is the product of isothermal solidification and no large precipitations have been noticed, some micron and submicron size voids were observed. For more detailed explanation, **Fig. 15** is given. In this figure, that is higher magnification of ISZ microstructure, some micron and Nano size precipitations can be noticed. According to the shapes of micron and Nano particles, it seems that these particles are silicide precipitations which do not have enough time to be solved in matrix or to be diffused to base metals.

The presence of these precipitations in ISZ confirms dimple fracture mechanism. On the other hand, because some precipitations are sub micro size, it can be concluded that the size of voids during plastic deformation decreases and causes dominant fracture mechanism not to be just dimple fraction. The presence of small size precipitations causes the size of voids to decrease, as a result of which shear strength increases.

Conclusions

The relation between microstructure and mechanical properties and fracture mechanism of IN718 / BNi-2 / AISI 316L joint was studied. The following conclusions can be drawn from this study:

(i) In Type I microstructure, it was observed that dominant fracture mechanism of this microstructure is dimple fracture. Despite the fact that bonding has been done at solid state on the one side, and the existence of rich components such as Ni, Cr, Si and B in the boning region on other side, it can be stated that formation of some hard borides/silicide precipitations within γ phase (that is nearly soft matrix) leads to dimple fracture.

(ii) In Type II microstructure, bonding temperature (1000℃) was enough, but not for bonding time, that led to formation of dual microstructure resulting from Athermal (eutectic and dendritic structure) and isothermal solidification. Eutectic regions are spiral islands created within isothermal solidification region. In fact, the main characteristic of this microstructure is the presence of hard and brittle eutectic phase within homogenous isothermal solidification microstructure. Existence of this hard phase within soft γ phase affects the ability of deformation γ phase that leads to quasi cleavage fracture. It is believed that quasi cleavage fracture mechanism occurred because of dual microstructure resulting from Athermal and isothermal solidification.

(iii) Type III microstructure, because of correct selection of time & bonding temperature (45 min and 1050^0C, respectively), achieved the single γ phase micro-structure. In addition to single γ phase homogenous microstructure, some sub-micron size precipitations with the same structure of silicide can be observed. Presence of these nanoscales precipitations does two vital jobs: first, these micron and sub-micron size precipitations cause combined dimples-tearing fracture mechanism. Second, they act as a strengthening mechanism that leads to increases in shear strength.

References

1. Shamsabadi, A. Y.; Bakhtiari, R.; G. E. B.; *J. Alloys Compd.,* **2016**, *685,* 896.
2. Pouranvari, M.; Ekrami, A.; Kokabi, A. H.; *Mater. Sci. Eng. A,* **2013**, *568,* 76.
3. Locci, I. E.; Bowman, C. L.; Gabbs, T. P.; Rd, B.; and Got, I. E. L.; "Development of High Temperature Dissimilar Joint Technology for Fission Surface Power Systems," Vol. 718. **2009**.
4. Bansal, A.; Sharma, A. K.; Das, S.; Kumar, P.; *Journal of Materials: Design and Applications,* **2016**, *230*, 939.
5. Devendranath Ramkumar, K.; et al., *J. Mater. Res.,* **2014**, *29*, 3011.
6. Davoodi, A.; Khorram, A.; Jafari, A.; *J. Manuf. Process.,* **2017,** *29,* 447.
7. Fezi, K.; Krane, M. J. M.; Nadakuduru, V. N.; Zhang, D. L.; Nair, B.G.; Winter, N.; "Development of a Novel Ni-Fe-Cr-B-Si Interlayer Material for Transient Liquid Phase Bonding of Inconel 718 Development of a Novel Ni-Fe-Cr-B-Si Interlayer Material for Transient Liquid Phase Bonding of Inconel 718," **2018**, pp. 0–8.
8. Pouranvari, M.; a. Ekrami, and a. H. Kokabi, *J. Alloys Compd.,* **2009**, *469,* 270.
9. Pouranvari, M.; Ekrami, A.; Kokabi, A. H.; Han, H. N.; *Int., Met. Mater.* **2013**, *19*, 1091.
10. Jost, W.; Diffusion in Solids, Liquids, Gases. Springer, 1969.
11. M. Pouranvari, A. Ekrami, and A. H. Kokabi, *J. Alloys Compd.*, **2013**, vol. 563, pp. 143–149,.
12. T. H. E. Volume, C. Were, D. Leroy, T. a Siewert, S. Liu, and G. R. Edwards, "Volume Handbook . the Volume Was Prepared Under the Direction of the Asm Handbook," Weld. Brazing Solder. **1993**, vol. 6, p. 2873.
13. Lippold, J. C.; Kiser, S. D.; DuPont, J. N.; Welding metallurgy and weldability of nickel-base alloys. John Wiley & Sons, 2011.
14. Davis, J. R.; "ASM specialty handbook: nickel, cobalt, and their alloys," ASM Int. Member/Customer Serv. Center, Mater. Park, **2000**. OH 44073-0002, USA, , pp. 7–13, **2000**.
15. Gray, D. E.; American institute of physics handbook. McGraw-Hill, 1982.